In-plane rotation of magnetic stripe domains in $Fe_{1-x}Ga_x$ thin films

S. Fin,[1] R. Tomasello,[2] D. Bisero,[1,3] M. Marangolo,[4] M. Sacchi,[4,5] H. Popescu,[5] M. Eddrief,[4] C. Hepburn,[4] G. Finocchio,[6] M. Carpentieri,[7] A. Rettori,[8,9] M. G. Pini,[10] and S. Tacchi[11,*]

[1]*Dipartimento di Fisica e Scienze della Terra, Università degli Studi di Ferrara, I-44122 Ferrara, Italy*

[2]*Department of Computer Science, Modelling, Electronics and System Science, University of Calabria, I-87036 Arcavacata di Rende (CS), Italy*

[3]*CNISM, Unità di Ferrara, I-44122 Ferrara, Italy*

[4]*Sorbonne Universités, UPMC Université Paris 06, UMR 7588, Institut des NanoSciences de Paris, 4 Place Jussieu, F-75005 Paris, France*

[5]*Synchrotron SOLEIL, B.P. 48, F-91192 Gif-sur-Yvette, France*

[6]*Department of Mathematical and Computer Sciences, Physical Sciences and Earth Sciences, V.le F. D'alcontres, 31, I-98166, Messina, Italy*

[7]*Department of Electrical and Information Engineering, Politecnico of Bari, I-70125 Bari, Italy*

[8]*Dipartimento di Fisica ed Astronomia, Università di Firenze, I-50019 Sesto Fiorentino (FI), Italy*

[9]*Centro S3, c/o Istituto Nanoscienze del CNR (CNR-NANO), Via Campi 213/a, I-41125 Modena, Italy*

[10]*Istituto dei Sistemi Complessi del CNR (CNR-ISC), Unità di Firenze, I-50019 Sesto Fiorentino (FI), Italy*

[11]*Istituto Officina dei Materiali del CNR (CNR-IOM), Unità di Perugia, c/o Dipartimento di Fisica e Geologia, Università di Perugia, I-06123 Perugia, Italy*

(Received 8 September 2015; revised manuscript received 10 November 2015; published 8 December 2015)

The in-plane rotation of magnetic stripe domains in a 65-nm magnetostrictive $Fe_{0.8}Ga_{0.2}$ epitaxial film was investigated combining magnetic force microscopy, vibration sample magnetometry, and x-ray resonant magnetic scattering measurements. We analyzed the behavior of the stripe pattern under the application of a bias magnetic field along the in-plane direction perpendicular to the stripe axis, and made a comparison with the analogous behavior at remanence. The experimental results have been explained by means of micromagnetic simulations, supported by energy balance considerations. Fields smaller than ∼400 Oe do not induce any stripe rotation; rather, a deformation of the closure domains pattern was evidenced. Larger fields produce a sudden rotation of the stripe structure.

DOI: 10.1103/PhysRevB.92.224411 PACS number(s): 75.70.−i, 75.30.Gw, 75.30.Ds, 75.60.Ch

I. INTRODUCTION

Magnetostrictive thin films of $Fe_{1-x}Ga_x$ (galfenol alloys) are currently the subject of a number of experimental investigations, particularly for their peculiar magnetic properties [1–4] and their applicative potential, e.g., in actuators and sensors [5] or microwave spintronics [6]. When epitaxially grown on a ZnSe/GaAs(001) substrate, $Fe_{1-x}Ga_x$ thin films present an enhanced magnetostriction as compared with pure Fe due to Ga-induced tetragonal distortion in the atomic arrangement [1,7]. Moreover epitaxial thin films present narrower resonant linewidths and lower damping with respect to sputtered samples [8]: i.e., two important characteristics for strain-controlled microwave and spin-wave applications [6].

Epitaxial $Fe_{1-x}Ga_x$ films with $0.15 < x < 0.29$, and thickness D larger than a critical value $D_c \sim 35$ nm, feature a regular pattern of stripes [2], alternating up and down magnetization components. The direction of the aligned stripes coincides with that of the last saturating field H_{sat}, applied parallel to the film surface [2,4]. Such a phenomenon, called "rotatable anisotropy," was first observed in vapor-deposited thin permalloy films [9]. Prosen *et al.* [9] proved that, in these films, it is possible to select the easy direction of the magnetization by the application of a sufficiently large magnetic field, showing that the resulting hysteresis curves are identical for any established easy axis. Later on, Fujiwara *et al.* [10] pointed out that the same phenomenon, observed in Ni, Fe, and Permalloy films with negative magnetostriction [11] and thickness greater than a critical value [11], is closely related to the presence of a magnetic stripe domain structure where the out-of-plane component of the magnetization has a periodic modulation.

Recently, the topic of "rotatable anisotropy" in ferromagnetic films with stripe domains gained renewed interest. On one hand, this was due to progress in theoretical understanding, both using models [12–14] and micromagnetic simulations [15–21]. On the other hand, several refined experimental techniques became available, both for magnetic domain visualization (such as magnetic force microscopy [2,3,22]) and for magnetization dynamics measurement (such as ferromagnetic resonance [23], or Brillouin light scattering [4]).

It is now widely accepted [12,13] that the physical origin of a stripe domain structure, characterized by a periodic modulation of the out-of-plane magnetization component lies in the energy competition between a moderate perpendicular magnetic anisotropy and the easy-plane dipole-dipole magnetostatic coupling. In order to observe a stripe domain structure in a film with quality factor $Q < 1$, the film thickness must be larger than a critical value [12,13]. We remind one that $Q = K_u/K_d$ is defined as the ratio between the uniaxial magnetic anisotropy energy K_u, favoring perpendicular magnetization, and the magnetic dipole-dipole energy, $K_d = 2\pi M_s^2$, where M_s is the saturation magnetization.

Finally, it is worth noticing the recent interest [24] for the domain structure in bulk $Fe_{1-x}Ga_x$ alloys. In fact, in single crystals with Ga percentages x =0.17 and 0.26, magnetization curves nearly nonhysteretic, and independent of the

*tacchi@fisica.unipg.it

crystallographic orientation ([100], [011], or [111]), were reported [24]. At the same time, the magnetostriction displayed [24] maxima along certain crystallographic directions in the (001) plane and, furthermore, was found not to conserve volume. Quite interestingly, all these phenomena could be reconciled in the frame of a peculiar micromagnetic structure, consisting in a highly periodic longitudinal and transverse cellular pattern of magnetic flux closure entities that were called "autarkic" [24], as they are magnetostatically and magnetoelastically self-sufficient (i.e., no magnetization nor strain is associated with each of them).

In this article, we study the in-plane rotation of stripe domains in a 65-nm thick epitaxial $Fe_{0.8}Ga_{0.2}$ film [4], combining different experimental techniques. Magnetic force microscopy (MFM) and vibrating sample magnetometry (VSM) measurements were performed applying a bias field H_{bias} in the direction perpendicular to the stripes, while x-ray resonant magnetic scattering (XRMS) measurements were used to probe the magnetization periodicity at remanence. The experimental results were analyzed using accurate micromagnetic simulations, supported by energy balance considerations. As long as H_{bias} is lower than a threshold value $H_{\text{thr}} \sim 400$ Oe, the stripe domain structure was found to gradually deform, expanding (shrinking) the flux closure cap domains, located at the two film surfaces, whose magnetization is favorably (unfavorably) oriented along H_{bias}, while the out-of-plane component of the magnetization does not change appreciably. As a consequence, the in-plane component of the magnetization along the bias field, measured by VSM, presents a linear increase as a function of H_{bias}, whereas the width and the period of the magnetic stripes remain almost unchanged in the MFM images. Moreover we found that, for $H_{\text{bias}} \geqslant H_{\text{thr}}$, the magnetic stripes start to rigidly rotate towards the field direction, reaching a complete reorientation at about H_{bias}=800 Oe. Finally, XRMS measurements indicate that such a deformation process is not completely reversible due to pinning effects.

II. EXPERIMENTAL SETUP AND MICROMAGNETIC MODELLING

The $Fe_{0.8}Ga_{0.2}$ film was deposited by co-evaporation from independent Fe and Ga Knudsen cell sources onto a ZnSe/GaAs(001) substrate in a molecular beam epitaxy chamber, following the procedure detailed in Ref. [1]. The epitaxy conditions were FeGa(001)‖ZnSe(001) and FeGa[100]‖GaAs[100]. The atomic Ga concentration was determined by x-ray photoelecton spectroscopy, while the film thickness ($D = 65$ nm) was determined by x-ray reflectometry. MFM images were recorded in the phase detection mode, using CoCr coated tips. We performed MFM measurements both at remanence, and in the presence of an in-plane static magnetic field of up to 800 Oe. Higher magnetic fields (up to 1 T) were used to saturate the sample in plane, in order to induce the formation of stripe domains along a given in-plane direction, stable at remanence. Static magnetization measurements were performed by VSM, in order to obtain the dependence of the magnetization component along an in-plane bias magnetic field of increasing intensity. XRMS measurements at the Fe-$L_{2,3}$ edges were performed at the Sextants beamline [25,26] of the Soleil synchrotron. In order to measure both the in-plane and out-of-plane periodicity of the stripe domain structure, rocking scans have been performed, using either σ or π linearly polarized light.

Micromagnetic simulations, based on the numerical solution of the Landau-Lifshitz-Gilbert (LLG) equation, have been performed by using a state-of-the-art parallel micromagnetic solver GPMagnet [21,27,28],

$$\frac{d\mathbf{m}}{d\tau} = -\mathbf{m} \times \mathbf{h}_{\text{eff}} + \alpha_G \mathbf{m} \times \frac{d\mathbf{m}}{d\tau}, \tag{1}$$

where $\mathbf{m}$ and $\mathbf{h}_{\text{eff}}$ are the FeGa normalized magnetization and the effective field, respectively; $\tau = \gamma_0 M_s t$ is the dimensionless time, γ_0 being the gyromagnetic ratio, M_s the saturation magnetization, and α_G the Gilbert damping factor. The effective field includes the exchange, magnetostatic, anisotropy, and external field contributions. The anisotropy field includes both the strong out-of-plane contribution and the small in-plane one [4]. The former favors the direction perpendicular to the film plane [i.e., the z axis in Fig. 5(a) later on], while the latter favors the ⟨110⟩ equivalent in-plane directions [i.e., the two orthogonal in-plane axes x and y in Fig. 5(a)]. We use a discretization cell of $3 \times 3 \times 6.5\,\text{nm}^3$ and we consider a reduced area with in-plane geometrical dimensions of 999×999 nm^2, whereas the assumed film thickness, 65 nm, is equal to the experimental one.

The parameters used in the simulations are as follows: exchange constant $A_{\text{ex}} = 1.6 \times 10^{-6}$ ergs/cm, $M_s = 1400$ emu/cm^3, in-plane anisotropy constant $K_1 = -0.8 \times 10^5$ ergs/cm^3, $\alpha_G = 0.1$. These values are equal to those previously used [4] to describe the $Fe_{0.8}Ga_{0.2}$ film. The out-of-plane anisotropy constant $K_u = 6.0 \times 10^6$ ergs/cm^3, instead, was considered as a free parameter, in order to reproduce the experimental value for the stripe period ($P \sim 100$ nm). We remark that, as theoretically predicted many years ago [12,13], and experimentally demonstrated in $Fe_{1-x}Ga_x$ films [2], the stripe pattern develops (for film thickness exceeding a critical value that depends on the Ga percentage) owing to the competition between the moderate out-of-plane anisotropy K_u, which favors the magnetization to lie perpendicularly to the film plane, and the easy-plane magnetic dipole-dipole interaction. The in-plane anisotropy [4] K_1, equally favoring two orthogonal in-plane directions, is a tiny remnant of the cubic anisotropy of Fe after doping by Ga atoms [2], and does not play an important role in the formation of stripe domains.

Thermal effects are included as an additional stochastic term to the effective field, computed as

$$\mathbf{h}_{\text{th}} = \frac{\xi}{M_s}\sqrt{\frac{2\alpha_G k_B T}{\gamma_0 \Delta V M_s \Delta t}}, \tag{2}$$

where k_B is the Boltzmann constant, ΔV is the volume of the computational cubic cell, Δt is the simulation time step, T is the temperature, and ξ is a Gaussian stochastic process. The thermal field $\mathbf{h}_{\text{th}}$ satisfies the following statistical properties:

$$\langle h_{\text{th},k}(\mathbf{r},t)\rangle = 0,$$

$$\langle h_{\text{th},k}(\mathbf{r},t) h_{\text{th},l}(\mathbf{r}',t')\rangle = F\delta_{k,l}\delta(t-t')\delta(\mathbf{r}-\mathbf{r}'), \tag{3}$$

where k and l represent the Cartesian coordinates x,y,z. According to that, each component of $\mathbf{h}_{\rm th} = (h_{{\rm th},x}, h_{{\rm th},y}, h_{{\rm th},z})$ is a space- and time-independent random Gaussian distributed number (Wiener process) with zero mean value [29,30]. The constant F measures the strength of thermal fluctuations and its value is obtained from the fluctuation-dissipation theorem [31].

III. RESULTS AND DISCUSSION

A. MFM

Figures 1(a)–1(h) show the stripe rotation imaged by MFM. The sample was initially saturated applying a 1-T external magnetic field along the [110] axis, producing a stripe domain structure along that direction. MFM images were recorded while applying an external field, $H_{\rm bias}$, of up to 660 Oe along the [1-10] direction. For each value of $H_{\rm bias}$, Fig. 1 shows two images, one obtained in the applied field [Figs. 1(a), 1(c), 1(e), and 1(g)], and the other after turning it off [Figs. 1(b), 1(d), 1(f), and 1(h)]. No significant difference is observed between the two kinds of images. This is confirmed by Fig. 1(i), where we compare the power spectral density (PSD) curves computed from the Fourier transform of the MFM images. Up to $H_{\rm bias} =$ 300 Oe, the stripes remain parallel to the [110] direction. Moreover, their period $P = 94$ nm is unchanged: See the position of the main peak in Fig. 1(i). At $H_{\rm bias} = 400$ Oe, the stripes start rotating towards the [1-10] axis and reach an almost complete reorientation at ∼700 Oe. We also performed the opposite rotation, preparing the stripes with their axis parallel to [1-10] and applying an increasing field along [110], and found the same behavior for the stripe rotation [32].

B. VSM

A typical longitudinal hysteresis loop measured by VSM along the [110] axis is displayed in Fig. 2 as a dashed red line. The coercive field is ∼150 Oe, and the remanent magnetization is $M_r/M_s \approx 0.5$. A region with a linear $M(H)$ dependence starts around 800 Oe, suggesting the presence of stripe domains [2], while in-plane saturation of the magnetization is achieved at $H_{\rm sat} \sim 1800$ Oe.

VSM measurements were performed also during the stripe rotation. First, the stripe domains were prepared following the same procedure used for the MFM measurements. Then, the magnetization was measured along the [1-10] direction while applying an increasing magnetic field, up to a maximum value $H_{\rm bias}$. Finally, the field was turned off for measuring the remanent magnetization $M_{\rm off}$.

This sequence was repeated for values of $H_{\rm bias}$ up to 2500 Oe, in steps of 100 Oe. Some of these minor loops are shown in Fig. 2 as black lines. It is worth noticing that the hysteresis loop recorded along [1-10] at the end of the above-described procedure was found to coincide with the hysteresis loop previously measured along [110] (dashed red line in Fig. 2).

Figure 3 shows the component of the magnetization parallel to the direction of the magnetic field versus $H_{\rm bias}$, measured both in the applied field (open black squares, $M_{\rm on}$) and at remanence (open red circles, $M_{\rm off}$). One can notice that the behavior of the two curves is rather different. When the

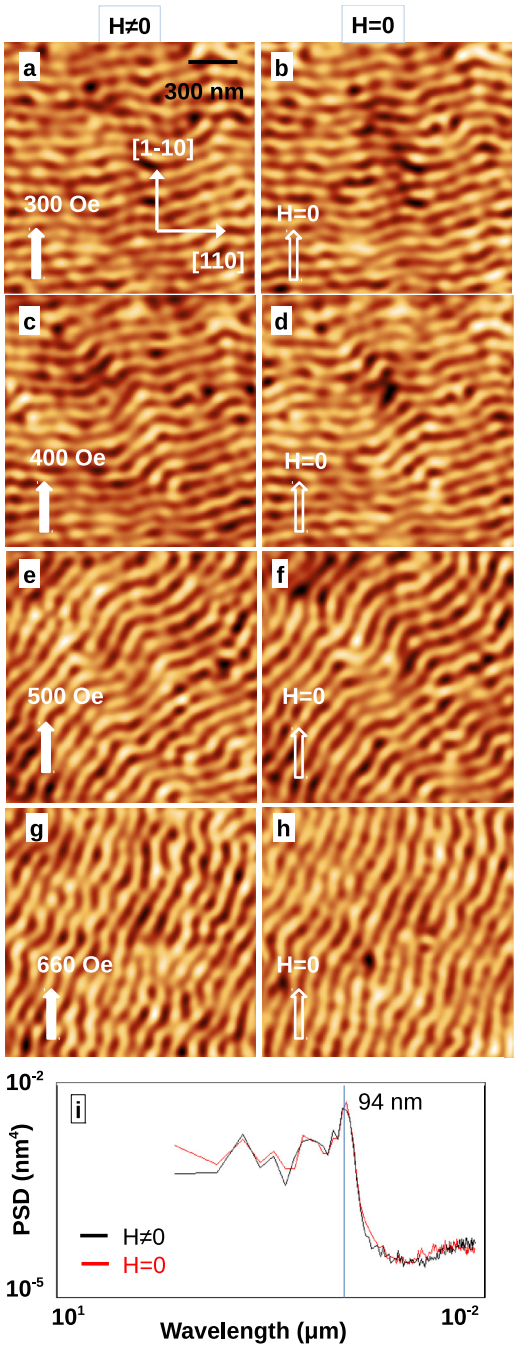

FIG. 1. (Color online) MFM images showing the rotation of stripes initially prepared along [110], due to the application of an increasing in-plane field along [1-10]. For each field value, two magnetic images were taken, one in the applied field (a), (c), (e), and (g), and the other after returning at remanence (b), (d), (f), and (h). (i) Comparison between the power spectral density (PSD) of the MFM images taken in an applied field of 300 Oe and at remanence.

magnetization component is recorded in the presence of the field, $M_{\rm on}$ presents a linear dependence on $H_{\rm bias}$, up to a threshold value $H_{\rm thr} \sim 400$ Oe. For larger fields, a noticeable reduction of the slope is found, indicating the onset of a new regime related to the rotation of the stripes, in agreement with the MFM measurements. A further reduction of the slope has

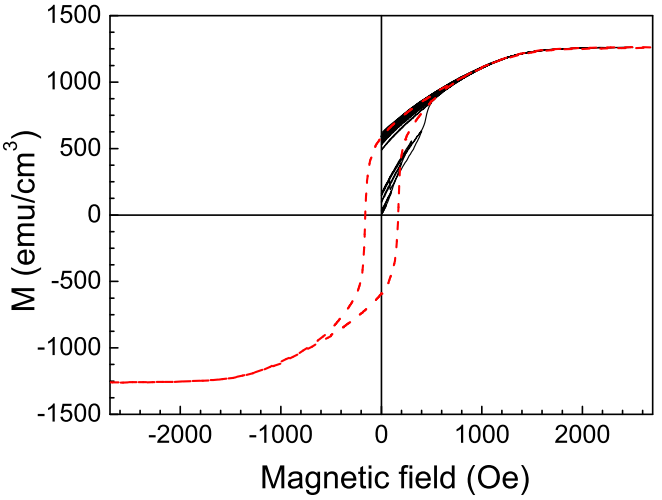

FIG. 2. (Color online) VSM longitudinal hysteresis loop (dashed red line) of the $Fe_{0.8}Ga_{0.2}$ film, measured along the in-plane [110] axis. Minor hysteresis loops (continuous black lines), measured by VSM applying a magnetic field along [1-10].

been observed for $H_{\text{bias}} \geqslant 800$ Oe, until the saturation value M_s is approached for $H_{\text{bias}} \geqslant H_{\text{sat}}$. When the magnetization component is recorded at remanence, a much smaller (but nonzero) increase of M_{off} is found for $H_{\text{bias}} < H_{\text{thr}}$. Such a behavior indicates that the process, occurring at small values of the bias field, is not totally reversible, probably due to pinning effects. In contrast, when $H_{\text{bias}} \geqslant H_{\text{thr}}$, due to the stripe rotation, M_{off} exhibits an abrupt increase, approaching the remanence value M_r.

C. XRMS

Figure 4(a) shows XRMS q_y-rocking curves measured using linearly polarized x rays tuned to the Fe-2p resonance

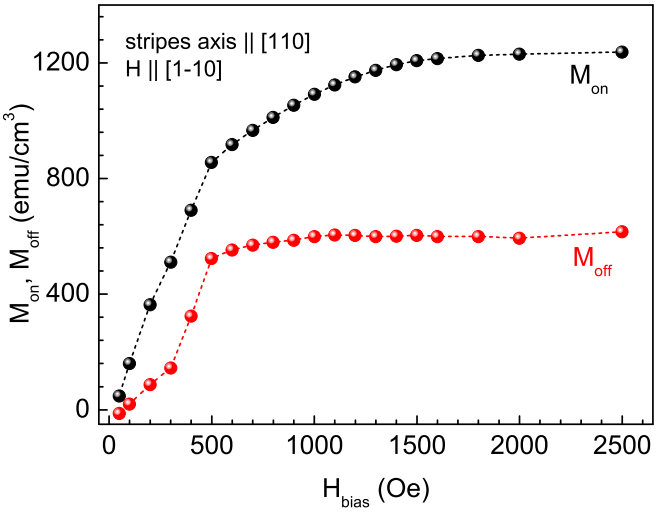

FIG. 3. (Color online) Component of the magnetization measured by VSM along the direction perpendicular to the stripes, as a function of H_{bias}. Black and red circles show measurements taken in the applied field (M_{on}) and at remanence (M_{off}), respectively. Dashed lines are guides to the eye.

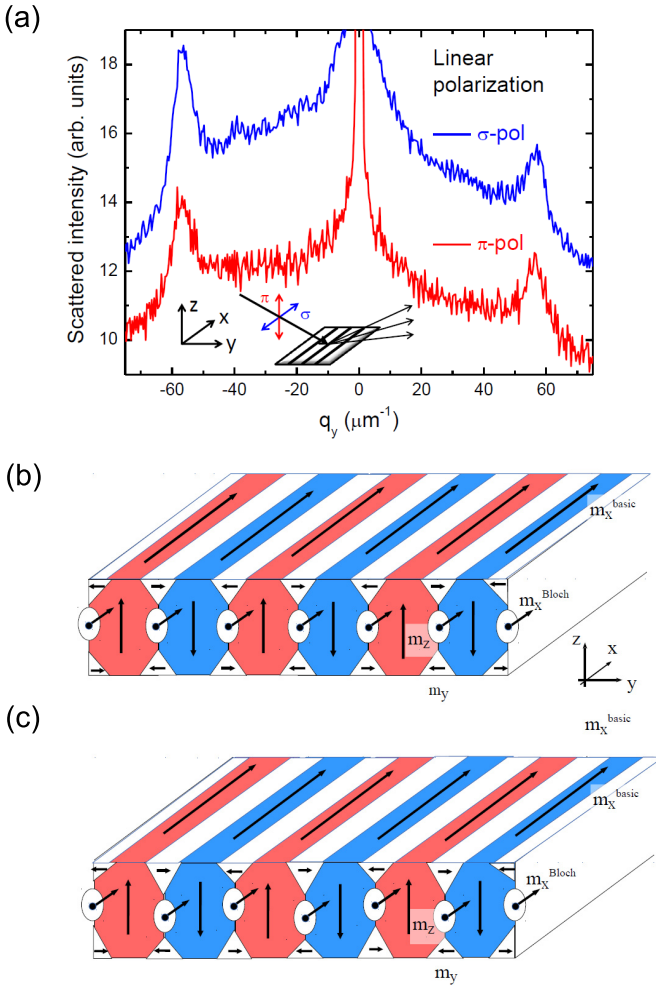

FIG. 4. (Color online) (a) Experimental XRMS rocking scans at the Fe-2p resonance with σ- and π-linear polarization. The inset shows the scattering plane (yz) perpendicular to the stripe axis ($x = [110]$). (b) and (c) Two possible schematic models of the magnetization configuration in the yz plane. Red/blue regions represent basic domains, with opposite values of the out-of-plane component m_z, while a substantial in-plane component m_x^{basic} is directed along the stripe axis. The white regions with elliptical section between two basic domains represent Bloch-like domains, with a small in-plane component m_x^{Bloch}. The white regions with triangular section located near the two film surfaces represent partial-flux-closure "cap" domains, with opposite values of the in-plane component m_y.

(707 eV). First, the stripes were aligned along the $x = [110]$ direction [normal to the yz scattering plane; see inset of Fig. 4(a)] by applying *ex situ* a 2 kOe static magnetic field. Prior to data collection, an alternating ±150 Oe (1-kHz frequency) bias field was applied *in situ* along the y=[1-10] direction, perpendicular to the stripes. Finally, q_y-rocking scans were performed at remanence using either σ- or π-linearly polarized light, in order to probe the periodicity of the three magnetization components of the film (M_x, M_y, M_z) along y.

The magnetic contribution to the scattering amplitude is proportional to the triple product $(\hat{\mathbf{e}}_{\text{out}} \times \hat{\mathbf{e}}_{\text{in}}) \cdot \mathbf{M}$ of the

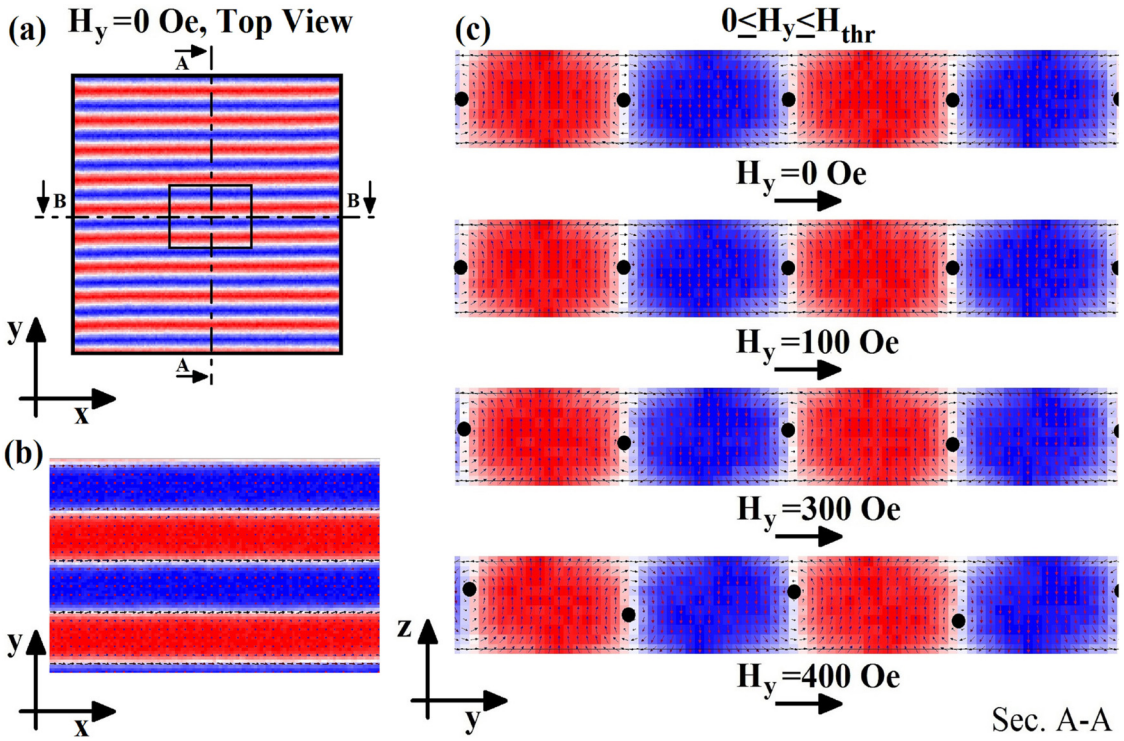

FIG. 5. (Color online) Micromagnetic simulation results. A color code is adopted for imaging M_z: Red regions have positive M_z, blue regions have negative M_z, and white regions have $M_z = 0$. (a) Top view of the film plane xy at zero field. The black rectangle delimits the central region of the film, for which the A-A section is displayed in Fig. 5(c). (b) Top view of the stripe domains in the central rectangular region of the film for $H_y = 0$. (c) Equilibrium magnetization configurations along the A-A section, calculated for different values of H_y. Black points denote the centers of the vortexlike configurations occurring in the yz plane for $H_y \leqslant H_{\text{thr}}$. Note that, owing to the finer discretization of the lateral film sides with respect to the film thickness, the horizontal-to-vertical aspect ratio is not preserved in the A-A sections.

incoming and outgoing polarization unit vectors with the magnetization. Therefore, using σ-polarized light ($\hat{\mathbf{e}}_{\text{in}} \| x$ and normal to the scattering plane), one probes the spatial modulations along the y direction of both M_y and M_z, while using π-polarized light ($\hat{\mathbf{e}}_{\text{in}}$ contained within the scattering plane) one probes the spatial modulations of the in-plane component M_x along the y direction.

As it can be seen in Fig. 4(a), the rocking scans are characterized, for both polarizations, by the presence of two peaks at $|q_\parallel| = 56.6\ \mu\text{m}^{-1}$, in addition to specular reflectivity. This indicates that all the magnetization components have a spatial periodicity $P \sim 111$ nm along the y direction. For σ-polarized light, the peaks correspond to the presence of partial-flux-closure "cap" domains with in-plane component m_y of alternating sign, located at the two film surfaces, in addition to the basic domains, with opposite values of the out-of-plane component m_z [Fig. 4(b)]. Note that, owing to the moderate quality factor ($Q \sim 0.49$ using the above mentioned FeGa parameters), basic domains have also a substantial in-plane component [m_x^{basic} in Fig. 4(b)], which is parallel to the direction of the last saturating field. Concerning the measurements with π-polarized light, it should be noticed that the in-plane component M_x presents an additional contribution from the Bloch-like domain walls [m_x^{Bloch} in Fig. 4(b)], besides the conventional one (m_x^{basic}).

As it can be seen in Fig. 4(b), for a domain structure with the M_y component fully compensated, M_x should have half the period of the M_y (or M_z) modulation. Therefore, the M_x modulation period observed by XRMS suggests that the Bloch-like domain walls shift alternately upwards and downwards along the z axis [Fig. 4(c)]. This result implies a pinning mechanism, which at remanence freezes the M_x component in an alternating upwards/downwards configuration, even after the external field has been removed. Moreover, we observe that also a pinning of the flux closure cap domains should be supposed, on the basis of the VSM data (see Fig. 3) which, for $H_{\text{bias}} < H_{\text{thr}}$, display a nonzero value of M_{off}. This implies that also the M_y component should freeze in an uncompensated, alternating right/left, configuration as the one in Fig. 4(c), even after the external field has been removed.

D. Micromagnetic simulations

The stripe domains pattern has been simulated by applying a strong magnetic field along the in-plane $+x$ axis (corresponding to the [110] direction of the sample) and then removing it. Figures 5(a) and 5(b) show top views of the simulated $Fe_{0.8}Ga_{0.2}$ film plane (xy) for $H_y = 0$, while snapshots of section A-A in the yz plane are reported in Fig. 5(c). At remanence, the stripe domain structure consists of basic domains, alternately magnetized up and down (along the z axis) with respect to the surface plane, and separated by Bloch-like domain walls, in-plane magnetized along the $+x$ direction. This leads to stripe domains, parallel to the saturation field and having a period $P = 90$–100 nm. Due to the moderate value of the out-of-plane anisotropy, the flux closure cap

domains consist of regions located near the film surface and in-plane magnetized along the y direction. Since such domains have equal size and are alternately magnetized, we found that at remanence the M_y component of the magnetization along the direction perpendicular to the stripes is zero, in agreement with the VSM results. Moreover, one can note that, at remanence, the period of the modulation for the in-plane component M_y is $W = P/2$, namely it is equal to the semiperiod of the modulation for the out-of-plane component M_z.

To simulate the domains rotation, a magnetic field has been applied in plane perpendicular to the stripes, along the y direction. The intensity of H_y has been increased from 0 to 2500 Oe by steps of 100 Oe or 500 Oe, depending on the range of H_y. Although the strong pinning effect induced by the boundaries of the simulated geometry prevents a quantitative comparison, the micromagnetic simulations can qualitatively explain the experimental results. When a small magnetic field is applied, the basic domains, which are out-of-plane magnetized, remain nearly unchanged. Therefore the stripe domains, and as a consequence the MFM pattern, are not altered in their structure. On the contrary, the flux closure cap domains with in-plane magnetization component m_y parallel (antiparallel) to the field direction, expand (shrink). As a consequence, the component of the magnetization parallel to the external field M_y linearly increases with H_y, in agreement with the VSM measurements performed in the applied field. Moreover, the centers of Bloch-type domain walls (i.e., black points at the center of vortexlike configurations in the yz plane) were found to shift, alternately upwards and downwards along the z direction, by almost half the height of a cell, for a 100 Oe increase of H_y in the range from 0 to 400 Oe. It is important to note that, in this low field regime, we found that these processes are totally reversible. Comparing Figs. 4(c) and 5(c), one can see that the micromagnetic simulations corroborate the presence of a pinning mechanism involving both the flux closure cap domains and the Bloch-like domain walls, in the low field range. When the intensity of the magnetic field is further increased above 400 Oe, the stripes start rotating towards the applied field direction, as it can be seen in Fig. 6(a), until, for $H_y = 2500$ Oe, the stripe axis achieves an almost complete reorientation along the y direction (the misalignment is $\approx 16^\circ$). Such a rather high value of the reorientation field is due to the pinning effect of the corners on the simulation. In Fig. 6(b), where both sections A-A and B-B are shown, it can be observed that, at this value of the field, the magnetization is almost uniform along the $+z$ direction in section A-A, while the complex structure consisting of basic domains, flux closure cap domains and Bloch-type domain walls is present in section B-B. In agreement with the MFM measurements, we found that during the rotation, the period of the stripe pattern remains almost constant.

E. Energy balance considerations using a simplified model for the stripes

In order to qualitatively explain the behavior of the stripe domain, the effect of a moderate bias field on the total free energy density has been analyzed, using a simplified model of the magnetic pattern. At remanence ($H_y = 0$) this model is shown in Fig. 7(a). It consists of basic domains having the same thickness D as the FeGa film, and period $P = 2W$; Bloch-like domain walls, schematized as ellipsoidal prisms of sectional area S_e, perimeter p_e, and length L; and partial-flux-closure domains, schematized as isosceles triangular prisms with basis B, height A, and length L. The stripe length L is supposed to be very large. When a small magnetic field, $0 < H_y < H_{\rm thr}$, is applied in-plane along a direction perpendicular to the stripe axis (x), we assume, as shown in Fig. 7(b), the favorably oriented triangular prisms to expand (basis $B_1 > B$, height $A_1 > A$) and the unfavorably oriented ones to shrink (basis $B_2 < B$, height $A_2 < A$), with no change in the prism length L because the stripes are supposed to be very long. In contrast, the Bloch-like domain-wall regions of elliptic sectional area S_e are supposed not to deform, but just to shift upwards or downwards along the z direction. For the partially deformed structure depicted in Fig. 7(b), the total magnetic free energy density (i.e., per unit area of the film WL), $f_{\rm tot} = f_w + f_d + f_u + f_Z$, can be estimated as follows.

(i) Wall energy density f_w. This contribution is obtained by multiplying the surface energy per unit area, $\sigma_w = 4\sqrt{K_u A_{\rm ex}}$, by the total area of the interfaces between different domains, and dividing by the unit film area WL. Denoting by p_e the perimeter of the ellipse, one has

$$f_w = \frac{\sigma_w}{W}\left[p_e + 2\sqrt{A_1^2 + \left(\frac{B_1}{2}\right)^2} + 2\sqrt{A_2^2 + \left(\frac{B_2}{2}\right)^2}\right]. \quad (4)$$

(ii) Magnetostatic energy density f_d. The higher is the quality factor Q of the film, more favored is an open domain structure. In the limit $B/W \to 0$, the open-flux Kittel domain configuration [34] is characterized by a high magnetostatic free energy density, $f_{d,\rm K} = 1.705(\frac{K_d}{2\pi})W$, for two equivalent film surfaces. In the opposite limit $B/W \to 1$ and $A = B/2$ (i.e., both angles at the basis of the isosceles triangle are equal to 45°), the flux closure Landau domain configuration has zero magnetostatic free energy density $f_{d,\rm L} = 0$. In the intermediate case of a partially open model ($0 < B/W < 1$), the magnetostatic free energy density is approximately given by [33]

$$f_d = \frac{4WK_d}{\pi^3}\sum_{n=0}^{\infty}\frac{\left[1 - e^{-(2n+1)\pi\frac{D}{W}}\right]}{(2n+1)^3} \times \left\{\cos^2\left[\frac{(2n+1)\pi}{2}\frac{B_1}{W}\right] + \cos^2\left[\frac{(2n+1)\pi}{2}\frac{B_2}{W}\right]\right\}, \quad (5)$$

where we have taken into account separately the contributions from two closure domains on opposite film surfaces [i.e., two triangular prisms, respectively, with basis B_1 and B_2; see Fig. 7(b)]. In the case of the domain structure in Fig. 7, the magnetization is not saturated along z because there is a substantial in-plane component directed along the stripe axis, $m_x > 0$. Therefore, in Eq. (5) one has $K_d = 2\pi m_z^2$ (rather than $K_d = 2\pi M_s^2$, as usual [33]).

(iii) Out-of-plane anisotropy energy density f_u. This contribution is obtained multiplying the constant K_u by the volume of the regions with magnetization not directed along the easy axis ($\pm z$), and dividing by the unit film area WL. Considering the Bloch-like domain wall region with sectional area S_e, and

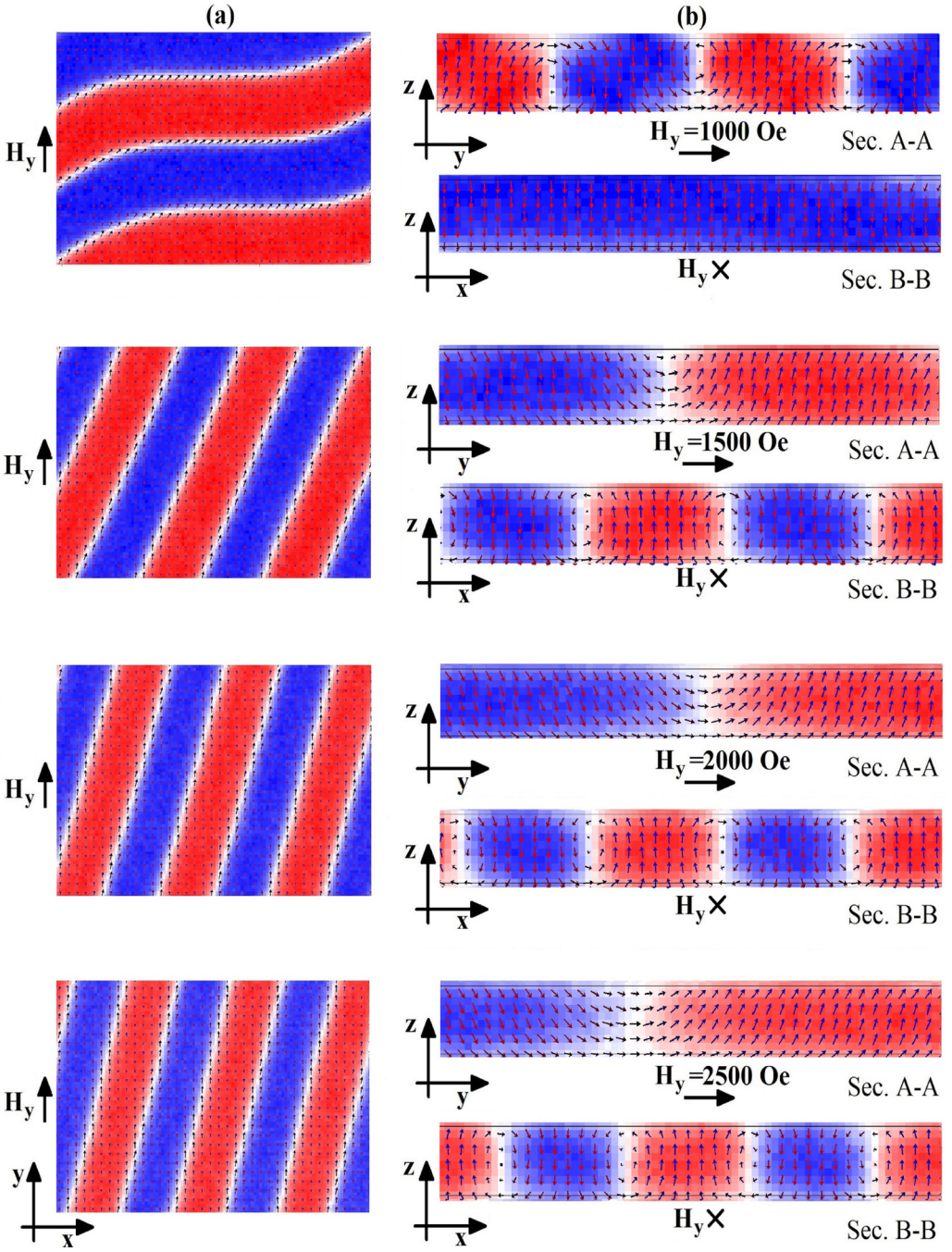

FIG. 6. (Color online) Micromagnetic simulation results of the $Fe_{0.8}Ga_{0.2}$ film for $H_y > H_{thr}$, showing the rotation of stripe domains. With reference to Fig. 5(a), the equilibrium magnetization configurations are shown (a) as a top view of the film plane xy and (b) along the A-A and B-B sections defined in Fig. 5(a). The different values of H_y are displayed just in (b).

the two different triangular prism regions located at the upper and the lower film surface, one thus obtains

$$f_u = \frac{K_u}{W}\left(S_e + \frac{B_1 A_1}{2} + \frac{B_2 A_2}{2}\right). \tag{6}$$

(iv) Zeeman energy density f_Z. This contribution comes from the two "cap" domain regions with opposite magnetization and takes the form,

$$f_Z = -\frac{H_y m_y}{W}\left(\frac{B_1 A_1}{2} - \frac{B_2 A_2}{2}\right), \tag{7}$$

where m_y is the magnetization in each triangular-prism region.

With the aim of further simplifying the model, we have expressed f_{tot} in terms of just one parameter δ. Namely, the basis of the two triangular sections of the closure domains were assumed to expand/shrink according to

$$B_1 \approx B(1+\delta), \quad B_2 \approx B(1-\delta), \tag{8}$$

respectively. Moreover, for the sake of simplicity, we assumed both angles at the basis of each isosceles triangle to be 45°, both in zero and applied field, so that $A \approx B/2$, $A_1 \approx B_1/2$,

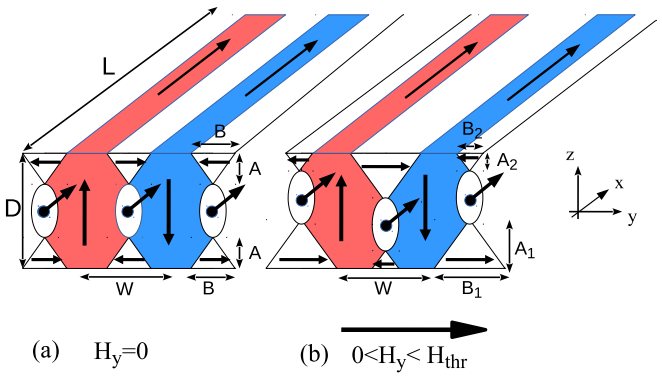

FIG. 7. (Color online) Schematic view of the domain configuration, with indication of the various lengths exploited in the energy balance considerations. (a) For $H_y = 0$, the domain structure includes basic domains, Bloch-type domains, and partial-flux-closure "cap" domains with the same volume and magnetization on both surfaces. (b) For $0 < H_y < H_{\rm thr}$, we assume (i) a deformation of the "cap" domains, in order that favorably (unfavorably) oriented regions expand (shrink), and (ii) a shift of the Bloch-type domains, upwards and downwards along the z direction, without deformation.

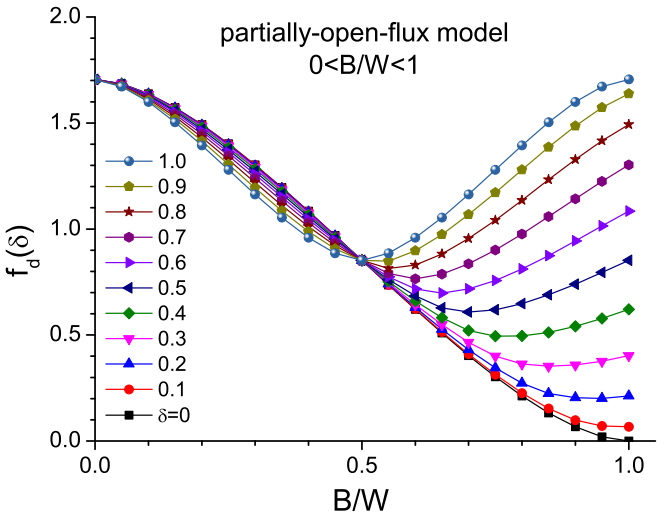

FIG. 8. (Color online) Magnetostatic energy density $f_d(\delta)$, expressed in units of $(\frac{K_d}{2\pi})W$, as calculated versus the ratio B/W for a partially open-flux model [see Eq. (10)] at selected values of the parameter δ.

$A_2 \approx B_2/2$. Therefore, in this approximation one has $A_{1,2} \approx A(1 \pm \delta)$, meaning that δ represents not only the percentual expansion/shrinkage of the triangle basis in the film section, but also the percentual shift (upwards or downwards along the z direction) of the vortex core in the elliptic section. In this way, one obtains the approximated total free energy density $f_{\rm tot}(\delta)$ as the sum of four contributions,

$$f_w \approx \frac{\sigma_w}{W}[p_e + 2\sqrt{2}B], \tag{9}$$

$$f_d(\delta) \approx \frac{4WK_d}{\pi^3}\sum_{n=0}^{\infty}\frac{[1-e^{-(2n+1)\pi\frac{D}{W}}]}{(2n+1)^3} \times\left\{\cos^2\left[\frac{(2n+1)\pi}{2}\frac{B}{W}(1+\delta)\right] + \cos^2\left[\frac{(2n+1)\pi}{2}\frac{B}{W}(1-\delta)\right]\right\}. \tag{10}$$

$$f_u(\delta) \approx \frac{K_u}{W}\left[S_e + 2(1+\delta^2)\left(\frac{B}{2}\right)^2\right], \tag{11}$$

$$f_Z(\delta) \approx -\frac{H_y m_y}{W}\left[4\delta\left(\frac{B}{2}\right)^2\right]. \tag{12}$$

Namely, within this approximated model, one has that (i) the wall energy density f_w does not depend on δ [see Eq. (9)]; (ii) the magnetostatic energy density f_d has a complicated behavior [see Eq. (10) and Fig. 8 later on]; (iii) the out-of-plane anisotropy energy density f_u increases on increasing δ [see Eq. (11)]; (iv) the Zeeman energy density f_Z decreases on increasing δ [see Eq. (12)].

In Fig. 8 we plot the magnetostatic energy density f_d in Eq. (10) versus B/W for selected values of δ. In the limit $B/W \to 0$, one recovers the completely open-flux (Kittel) model [34], and the magnetostatic energy assumes the maximum value $f_{d,\rm K} = 1.705(\frac{K_d}{2\pi})W$, whatever the value assumed by the parameter δ. In contrast, for a partially open-flux model ($0 < B/W < 1$), f_d does depend on δ. When $B/W < 0.5$, f_d smoothly decreases on increasing δ, whereas, if $B/W > 0.5$, f_d rapidly increases with δ. In the special case $B/W = 0.5$, f_d is independent of δ.

When an external field is applied, the deformed equilibrium configuration can be obtained minimizing the total free energy density $f_{\rm tot}(\delta)$ with respect to the parameter δ. We performed the minimization of $f_{\rm tot}(\delta)$, assuming different values for the B/W ratio. When B/W comprises a reasonable range from 0.4 to 0.6, we numerically found [35] the equilibrium value of the percentual upwards/downwards shift of a vortex core to increase almost linearly with the bias field, $\delta_{\rm eq} \propto H_y$. This result allows us to qualitatively justify the linear dependence of $M_{\rm on}$ versus the bias field for $H_y < H_{\rm thr}$. In fact, in our approximated model, the component of the film magnetization along H_y is simply given by

$$M_{\rm on} = M_y = \frac{V_1 - V_2}{V_1 + V_2}m_y = \frac{2\delta_{\rm eq}}{1+\delta_{\rm eq}^2}m_y, \tag{13}$$

where V_1 (V_2) is the volume of a favorably (unfavorably) oriented "cap" domain, and m_y is the magnetization in each triangular-prism region. For low field values, from (13) one can conclude that $M_{\rm on} \propto H_y$, in qualitative agreement with VSM data (see Fig. 3).

IV. CONCLUSIONS

In summary, we have investigated the stripe domains rotation in a 65-nm magnetostrictive $Fe_{0.8}Ga_{0.2}$ film, by means of MFM and VSM measurements performed under application of a bias magnetic field $H_{\rm bias}$ in the direction perpendicular to the stripes. When the intensity of $H_{\rm bias}$ is smaller than a threshold value $H_{\rm thr} \cong 400$ Oe, the in-plane component of the magnetization, measured along the direction perpendicular to the stripes, exhibits a linear increase as a function of $H_{\rm bias}$, whereas no apparent change of the stripe domains structure

is observed by MFM. These results have been explained on the basis of micromagnetic simulations, supported by energy balance considerations. It has been found that for low values of H_{bias}, the stripe domain structure deforms expanding/shrinking the partial-flux-closure cap domains, depending on their favorable/unfavorable orientation with respect to the applied field direction, while the out-of-plane component of the magnetization in the basic domains does not change appreciably. Such a deformation gradually develops up to a threshold field $H_{\text{thr}} \cong 400$ Oe. It is worth noticing that both VSM and XRMS measurements at remanence suggest that, in the real system, the deformation process is not totally reversible, on removing the external field, most probably owing to pinning effects. For $H_{\text{bias}} \geqslant H_{\text{thr}}$, the magnetic stripes start rotating towards the field direction. In agreement with the MFM measurements, we found that the period of the stripe pattern remains almost constant during the rotation. These results provide a further step towards the understanding of the stripe domains properties and offer useful information for the development of $Fe_{1-x}Ga_x$-based magnetostrictive devices.

ACKNOWLEDGMENTS

Support from the Ministero Italiano dell'Università e della Ricerca (MIUR) under the PRIN2010 Project (No. 2010ECA8P3) and FIRB2010 (No. RBFR10E61T). Support from CNR (Italy) and CNRS (France) under collaborative Project No. PICS-2013 "SWIM" and by Agence Nationale pour la Recherche (France) under Grant No. 13-JS04-0001-01 "SPINSAW" is gratefully acknowledged. We thank Luis Torres and Javier Gomez Martin for the software support to the micromagnetic simulations; Edgar Bonfiglioli for help with the LabView software; and Giovanni Carlotti and Julià Milano for fruitful discussions and suggestions.

[1] M. Eddrief, Y. Zheng, S. Hidki, B. Rache Salles, J. Milano, V. H. Etgens, and M. Marangolo, Phys. Rev. B **84**, 161410(R) (2011).
[2] M. Barturen, R. Rache Salles, P. Schio, J. Milano, A. Butera, S. Bustingorry, C. Ramos, A. J. A. de Oliveira, M. Eddrief, E. Lacaze, F. Gendron, V. H. Etgens, and M. Marangolo, Appl. Phys. Lett. **101**, 092404 (2012).
[3] M. Barturen, M. Sacchi, M. Eddrief, J. Milano, S. Bustingorry, H. Popescu, N. Jaouen, F. Sirotti, and M. Marangolo, Eur. Phys. J. B **86**, 191 (2013).
[4] S. Tacchi, S. Fin, G. Carlotti, G. Gubbiotti, M. Madami, M. Barturen, M. Marangolo, M. Eddrief, D. Bisero, A. Rettori, and M. G. Pini, Phys. Rev. B **89**, 024411 (2014).
[5] B. Adolphi, J. McCord, M. Bertram, C.-G. Oertel, U. Merkel, U. Marschner, R. Schäfer, C. Wenzel, and W.-J. Fischer, Smart Mater. Struct. **19**, 055013 (2010).
[6] D. E. Parkes, L. R. Shelford, P. Wadley, V. Holy, M. Wang, A. T. Hindmarch, G. van der Laan, R. P. Campion, K. W. Edmonds, S. A. Cavill, and A. W. Rushforth, Sci. Rep. **3**, 2220 (2013).
[7] M. Barturen, J. Milano, M. Vásquez-Mansilla, C. Helman, M. A. Barral, A. M. Llois, M. Eddrief, and M. Marangolo, Phys. Rev. B **92**, 054418 (2015)
[8] E. M. Summers, T. A. Lograsso, and M. Wun-Fogle, J. Mater. Sci. **42**, 9582 (2007).
[9] R. J. Prosen, J. O. Holmen, and B. E. Gran, J. Appl. Phys. **32**, S91 (1961).
[10] H. Fujiwara, Y. Sugita, and N. Saito, Appl. Phys. Lett. **4**, 199 (1964).
[11] S. S. Lehrer, J. Appl. Phys. **34**, 1207 (1963).
[12] Y. Murayama, J. Phys. Soc. Jpn. **21**, 2253 (1966).
[13] L. M. Alvarez-Prado, G. T. Perez, R. Morales, F. H. Salas, and J. M. Alameda, Phys. Rev. B **56**, 3306 (1997).
[14] S. M. Ryabchenko, V. M. Kalita, M. M. Kulik, A. F. Lozenko, V. V. Nevdacha, A. N. Pogorily, A. F. Kravets, D. Y. Podyalovsky, A. Ya. Vovk, R. P. Borges, M. Godinho, and V. Korenivski, J. Phys.: Condens. Matter **25**, 416003 (2013).
[15] M. Labrune and J. Miltat, J. Appl. Phys. **75**, 2156 (1994).
[16] M. Labrune and L. Belliard, Phys. Status Solidi A **174**, 483 (1999).
[17] M. Labrune and A. Thiaville, Eur. Phys. J. B **23**, 17 (2001).
[18] N. Vukadinovic, O. Vacus, M. Labrune, O. Acher, and D. Pain, Phys. Rev. Lett. **85**, 2817 (2000); N. Vukadinovic, H. Le Gall, J. Ben Youssef, V. Gehanno, A. Marty, Y. Samson, and B. Gilles, Eur. Phys. J. B **13**, 445 (2000); N. Vukadinovic, M. Labrune, J. Ben Youssef, A. Marty, J. C. Toussaint, and H. Le Gall, Phys. Rev. B **65**, 054403 (2001).
[19] L. M. Alvarez-Prado and J. M. Alameda, Physica B **343**, 241 (2004).
[20] O. de Abril, M. del Carmen Sanchez, and C. Aroca, Appl. Phys. Lett. **89**, 172510 (2006).
[21] L. Lopez-Diaz, D. Aurelio, L. Torres, E. Martinez, M. A. Hernandez-Lopez, J. Gomez, O. Alejos, M. Carpentieri, G. Finocchio, and G. Consolo, J. Phys. D: Appl. Phys. **45**, 323001 (2012).
[22] E. Sallica Leva, R. C. Valente, F. Martinez Tabares, M. Vásquez Mansilla, S. Roshdestwensky, and A. Butera, Phys. Rev. B **82**, 144410 (2010).
[23] Wee Tee Soh, Nguyen N. Phuoc, C. Y. Tan, and C. K. Ong, J. Appl. Phys. **114**, 053908 (2013).
[24] H. D. Chopra and M. Wuttig, Nature (London) **521**, 340 (2015).
[25] M. Sacchi, H. Popescu, R. Gaudemer, N. Jaouen, A. Avila, R. Delaunay, F. Fortuna, U. Maier, and C. Spezzani, J. Phys.: Conf. Ser. **425**, 202009 (2013).
[26] M. Sacchi, N. Jaouen, H. Popescu, R. Gaudemer, J. M. Tonnerre, S. G. Chiuzbaian, C. F. Hague, A. Delmotte, J. M. Dubuisson, G. Cauchon, B. Lagarde, and F. Polack, J. Phys.: Conf. Ser. **425**, 072018 (2013).
[27] S. L. GoParallel, https://www.goparallel.net/index.php/gp-software (2012). Date of access: July 1, 2014.
[28] A. Giordano, G. Finocchio, L. Torres, M. Carpentieri, and B. Azzerboni, J. Appl. Phys. **111**, 07D112 (2012).
[29] W. F. Brown, Jr., Phys. Rev. **130**, 1677 (1963).
[30] D. M. Apalkov and P. B. Visscher, Phys. Rev. B **72**, 180405(R) (2005).
[31] H. B. Callen and T. A. Welton, Phys. Rev. **83**, 34 (1951).
[32] S. Fin, private communication; see also S. Fin, Ph.D thesis, University of Ferrara, Italy, 2014.
[33] A. Hubert and R. Schäfer, *Magnetic Domains: The Analysis of Magnetic Microstructures* (Springer, Berlin, 1998).
[34] C. Kittel, Phys. Rev. **70**, 965 (1946).
[35] We note that, in the particular case $B/W = 0.5$, the equilibrium value $\delta_{\text{eq}} = H_y m_y / K_u$ can be determined analytically because f_d does not depend on δ.